X-ray Pole Figures to Assess Orientation in PVC Sheets

Marianne Gilbert,[1] David H Ross,[1] Hwan Chul Kim[2]

[1]*Institute of Polymer Technology and Materials Engineering, Loughborough, Leicestershire LE11 3TU, United Kingdom*
[2]*Department of Textile Engineering, Chonbuk National University, Korea*

Received 22 November 2005; accepted 24 July 2006
DOI 10.1002/app.25544
Published online in Wiley InterScience (www.interscience.wiley.com).

ABSTRACT: A series of X-ray pole figures were obtained from oriented and unoriented rigid polyvinyl chloride sheets. From these, information about crystallite orientation in uniaxially and biaxially drawn sheets stretched at 90°C was obtained. Uniaxial orientation produced two crystallite orientations with the extent of orientation increasing with draw ratio; for biaxial samples the chain direction (c) was distributed uniformly in the plane of the sheet, with the planar orientation improving as draw ratio increased. © 2007 Wiley Periodicals, Inc. J Appl Polym Sci 104: 528–535, 2007

Key words: PVC; orientation; X-ray; pole figures

INTRODUCTION

Polyvinyl chloride (PVC) possesses about 10% crystallinity, which exists as small crystallites with a wide range of sizes and perfection. The amount of crystallinity and crystallite size is limited by the amount of syndiotacticity (typically 55%) in commercial suspension PVC. The unit cell in crystalline PVC was first investigated by Natta and Corradini. The cell is orthorhombic with dimensions $a = 1.06$ nm, $b = 0.54$ nm, and $c = 0.51$ nm.[1] Each cell contains two PVC chains arranged in planar zig-zag conformation, with the c direction corresponding to two chemical repeat units. Since lengths of syndiotactic sequences are on average no more than 5–6 repeat units,[2] crystallites in the c direction are very thin, consistent with the model proposed by Summers.[3] X-ray diffraction (XRD) traces for PVC were first published by Mammi and Nardi in 1963.[4] The amorphous trace for PVC consists of two broad diffraction peaks. The first one ($d = 0.36$ nm) is similar to that observed in most amorphous polymers, and corresponds to Van der Waals spacings between groups of atoms. The peak corresponding to $d = 0.50$ nm has been attributed to various types of chain packing in non crystalline regions.[4–7] For ''crystalline PVC'' three main diffraction peaks are observed, superimposed on the amorphous background. Using Cu K_α radiation, maxima are observed in the 16–18°2θ and 25°2θ regions (Fig. 1). The peaks at 16–18°2θ have been assigned to (110) and (200) planes, while at 25°2θ overlapping peaks from (210), (201), and (111) planes are present. Further details of XRD traces for PVC have been reviewed previously.[8] In oriented PVC products amorphous and crystallite orientation occurs, and mesomorphous structures are created, producing substantial improvements in mechanical properties at relatively low draw ratios[9,10] leading to increased usage in pressure pipes, for example. Pole figure analysis has previously been used in an attempt to obtain more detailed information on the crystallite orientation in uniaxially and biaxially oriented PVC sheets, thus improving the understanding of structure property relationships.[11,12] In this study further work carried out using improved instrumentation has provided new information about oriented crystalline structures.

EXPERIMENTAL

Rigid PVC sheet used was 1.0 mm thick Cobex 0680 supplied by Wardle Storeys. This is calendered sheet subsequently relaxed in a press to remove residual orientation. Using the BASE equipment as described previously,[9,10] samples were uniaxially drawn to draw ratios (DR) of 2.0 and 3.0, while being restrained in the transverse direction, and also equally biaxially drawn to 1.5 and 1.8. Wide angle XRD traces for these samples were obtained using a Bruker D8 X-ray diffractometer, with graphite monochromated Cu K_α radiation at 40 kV and 40 mA. Traces were recorded from 1–50°2θ, using a step size of 0.02°. XRD pole figures were also obtained on the Bruker D8 X-ray diffractometer with a Huber quarter circle eulerian cradle using Ni filtered Cu K_α radiation at 40 kV and 40 mA. Data were collected at selected 2θ angles for tilt angles χ every 5° between zero and 70°, and sample rotation angles ϕ at every

Correspondence to: M. Gilbert (m.gilbert@lboro.ac.uk).

Journal of Applied Polymer Science, Vol. 104, 528–535 (2007)

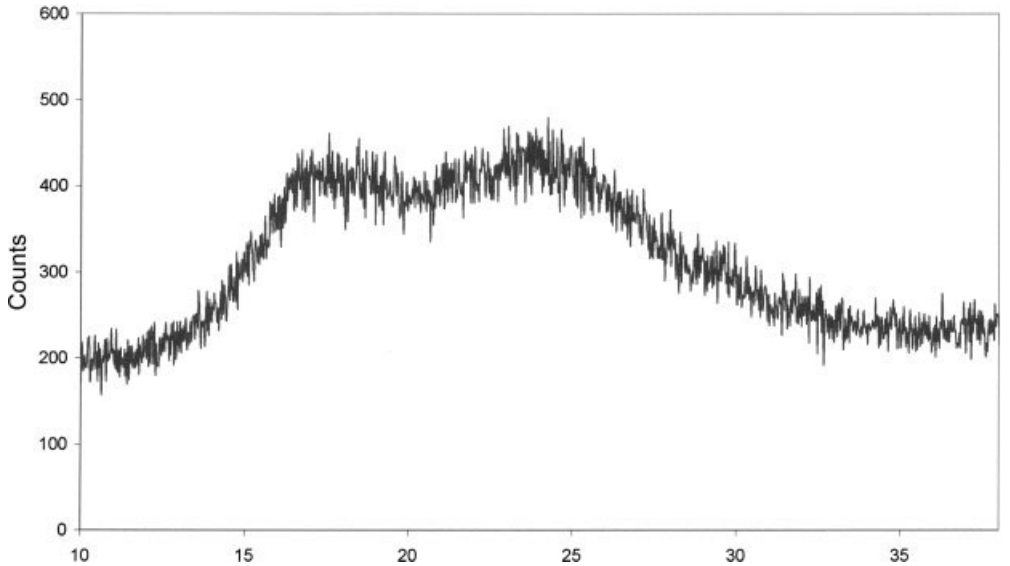

Figure 1 XRD trace for undrawn PVC sheet.

5° from 0° to 355°. Because the peaks are broad and not clearly separated from each other, the data from the wide angle plots points at 12° and 35°2θ were taken as representative background readings. Intensity values were measured at 12° and 35°2θ at a single ϕ angle for each χ angle for each set of plane measurements. The computer program interpolated each pair of background readings to give the relevant background reading for subtraction from the experimental values.

RESULTS

A wide angle XRD trace for an undrawn compression molded PVC sheet is shown in Figure 1. Wide angle diffraction traces for the sample uniaxially stretched to a draw ratio of 3.0, and biaxially stretched to 1.8 are shown in Figure 2(a,b). X-ray pole figures for the uniaxially and biaxially stretched sheets were obtained at 16.9, 18.7, and 24.8°2θ corresponding to maxima shown in Figure 1. These angles correspond to (200), (110) and overlapping peaks from (210), (201), and (111) reflections, respectively. In all pole figures, the relative intensities of the lines are as follows: black: red: blue: green: purple: red brown relate to 1 : 2 : 3 : 4 : 5 : 6. As figures are normalized, the colors do not relate to a specific number of counts, which differ in different figures. Pole figures for undrawn PVC sheet are shown in Figure 3. Inner circles correspond to χ angles from 0° to 70° from the sheet normal (SN). Figure 4 shows a set of pole figures for the sample biaxially drawn to a draw ratio of 1.8, and Figure 5 shows three-dimensional representations for the same sample. A full set for a sample uniaxially drawn (restrained in transverse direction) to a draw ratio of 3.0 is shown in Figure 6. In the pole figures, the north south direction corresponds to the stretch direction (MD), the west east direction corresponds to the transverse direction (TD), and the center of the pole figure corresponds to the SN. For the 3D representations, the south-west north-east line on the figures corresponds to the TD.

Figure 7 is a 3D representation of the pole figure in Figure 6(c), while Figures 8 and 9 use 3D representations of pole figures to illustrate the effect of increasing biaxial and uniaxial draw ratio on the orientation of the (200) planes.

DISCUSSION

As indicated earlier, PVC possesses an orthorhombic unit cell with dimensions $a = 1.06$ nm, $b = 0.54$ nm, and $c = 0.51$nm.[1] The polymer chain axis lies in the c direction, so is parallel to (200) and (110) planes. The broad peak around 25°2θ consists of three overlapping reflections as indicated; Guerrero et al.[13] showed that the relative intensity of these peaks was as follows, $I_{(210)} : I_{(201)} : I_{(111)}$ is 34.4 : 72.7 : 66.9 (relative values calculated on an arbitrary scale), so that this peak is primarily derived from planes which are not parallel to the chain axes (i.e., *c* direction).

For undrawn samples, (Fig. 3) there is some evidence of preferred orientation. Both (200) planes [Figs. 3(a) and 7(a)] and (110) planes [Fig. 3(b)] show a concentration of poles in the SN-MD which will be due to limited residual orientation remaining after processing. These pole figures indicate a tendency for *a* and *b* axes to lie in the SN-MD plane.

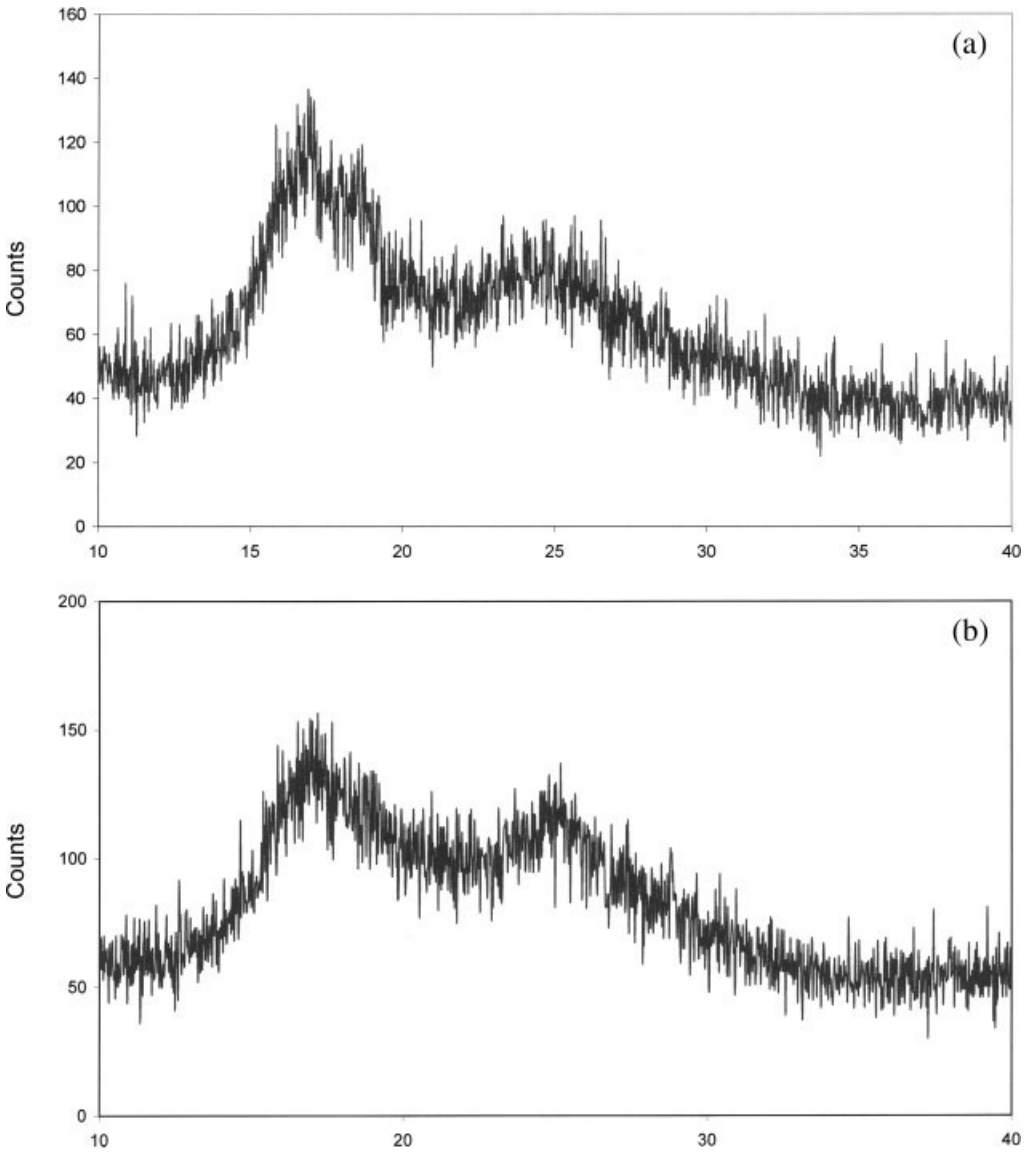

Figure 2 (a) XRD trace for uniaxially stretched PVC sheet. (b) XRD trace for biaxially stretched PVC sheet.

Figure 4(a) shows that for biaxially oriented (200) poles, i.e., *a* axes are concentrated in the SN direction, implying that b and the polymer chain axis *c* are distributed fairly uniformly in the plane of the film. This is seen very clearly in the corresponding 3D representation, Figure 5(a). Angles between (hkl) planes were calculated from the following equation for an orthorhombic unit cell,[14] and are listed in Table I.

$$\cos\phi = \frac{\frac{h_1h_2}{a^2} + \frac{k_1k_2}{b^2} + \frac{l_1l_2}{c^2}}{\sqrt{\left(\frac{h_1^2}{a^2} + \frac{k_1^2}{b^2} + \frac{l_1^2}{c^2}\right)\left(\frac{h_2^2}{a^2} + \frac{k_2^2}{b^2} + \frac{l_2^2}{c^2}\right)}} \quad (1)$$

The (110) poles lie at 63° to the (200) planes. There is some evidence of the presence of peak maxima at about 55° from the SN direction but uniformly distributed in the TD/MD plane in Figure 4(b), which could be consistent with the interpretation of the (200) pole figure. However, there are also elongated maxima lying from 25° to 40° from the SN in the SN/MD plane, probably associated with the frozen in orientation introduced during sheet production. The composite pole figure in Figure 4(c) also suggests that *b* and *c* axes are randomly distributed in the plane of the film, i.e., implying a fairly uniform planar distribution of polymer chains.

Results for uniaxially drawn samples (Fig. 6) are very different. On drawing, two distributions of *a* axis poles [Fig. 6(a)] are observed with maxima in the SN direction, but also in the SN/TD plane, with a maximum at 35° to the SN direction. These additional maxima are again shown more clearly in the 3D representations, Figure 8(b,c). In (110) pole fig-

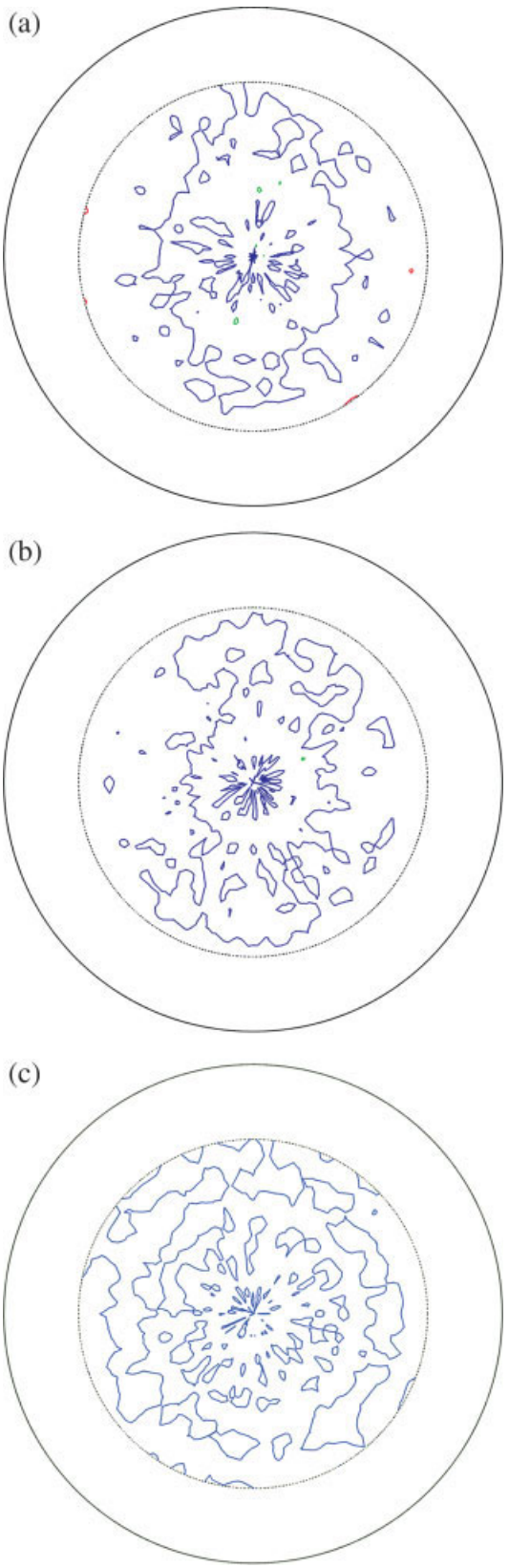

Figure 3 Pole figures for undrawn PVC sheet (a) 200; (b) 110; (c) 210, 201, 111. [Color figure can be viewed in the online issue, which is available at www.interscience.wiley.com.]

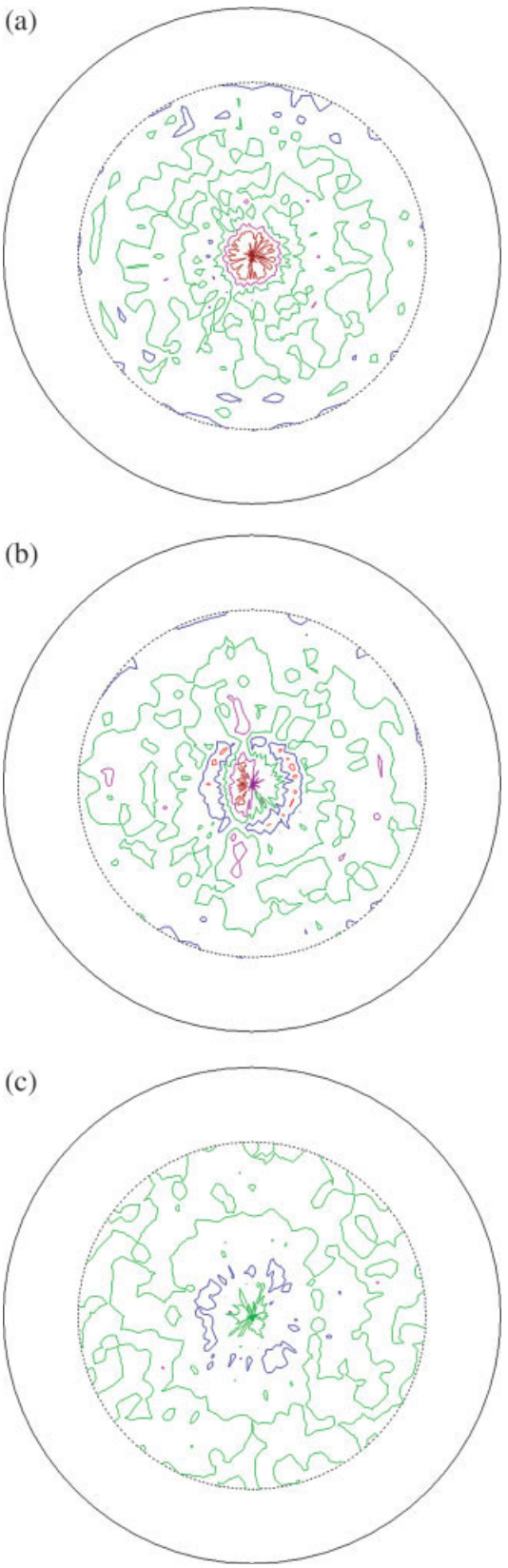

Figure 4 Pole figures for biaxially oriented PVC sheet (a) 200; (b) 110; (c) 210, 201, 111. [Color figure can be viewed in the online issue, which is available at www.interscience.wiley.com.]

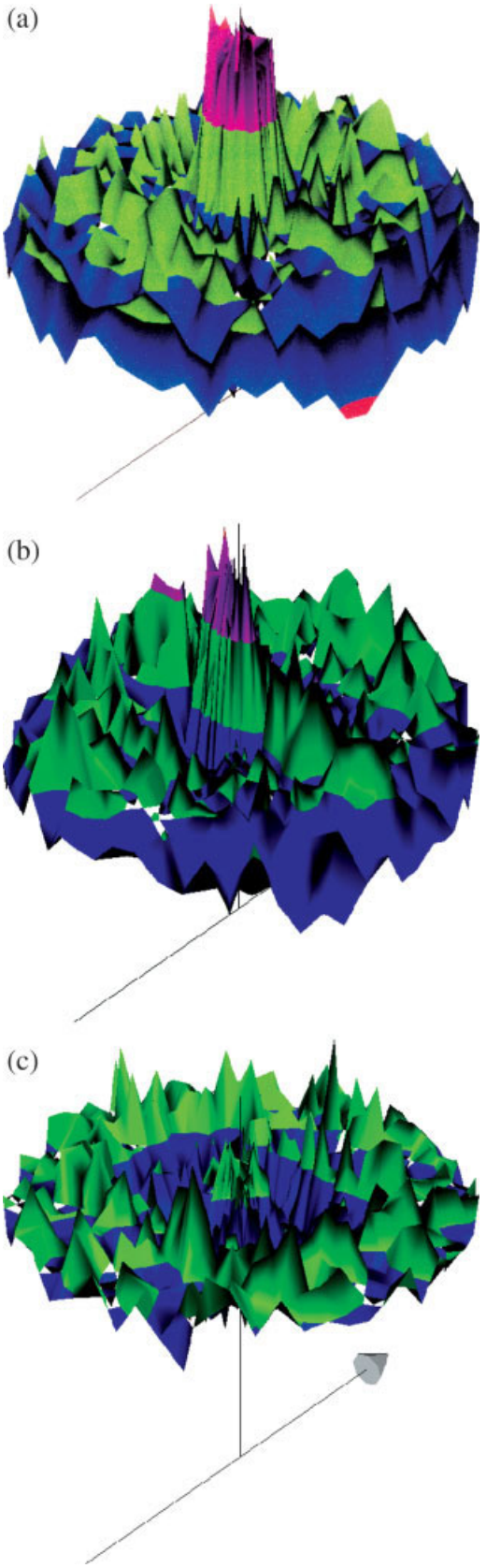

Figure 5 Three dimensional representation for biaxial sample DR = 1.8. (a) 200; (b) 110; (c) 210, 201, 111. [Color figure can be viewed in the online issue, which is available at www.interscience.wiley.com.]

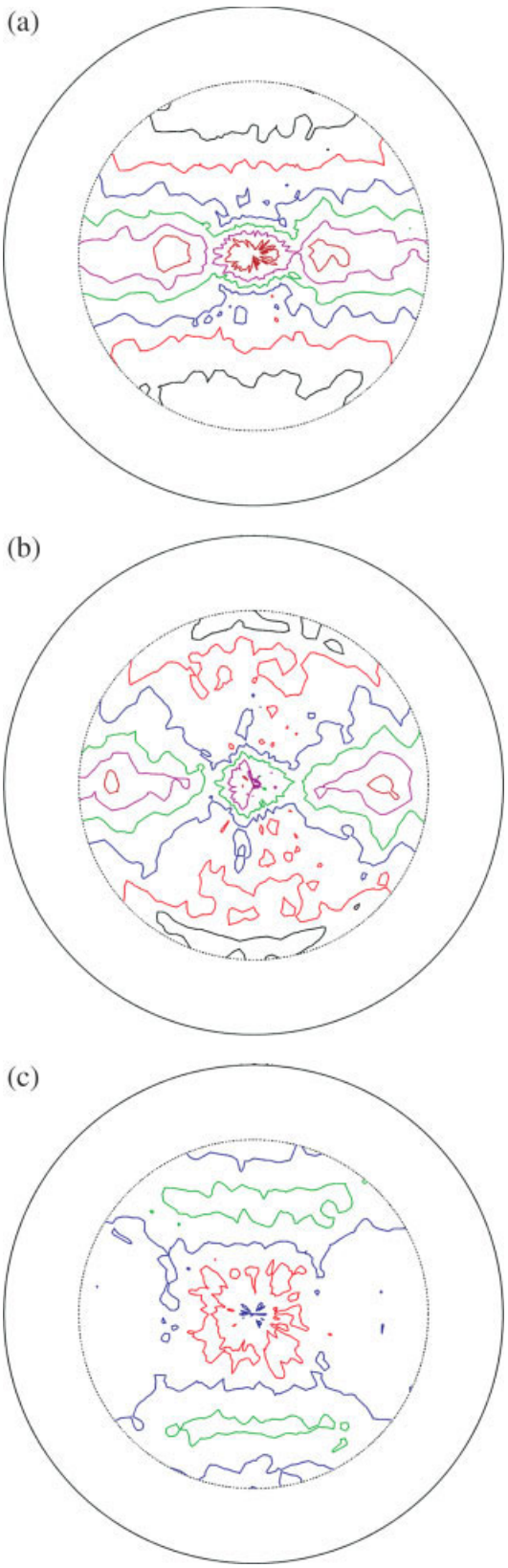

Figure 6 Pole figures for uniaxially oriented PVC sheet (a) 200; (b) 110; (c) 210, 201, 111. [Color figure can be viewed in the online issue, which is available at www.interscience.wiley.com.]

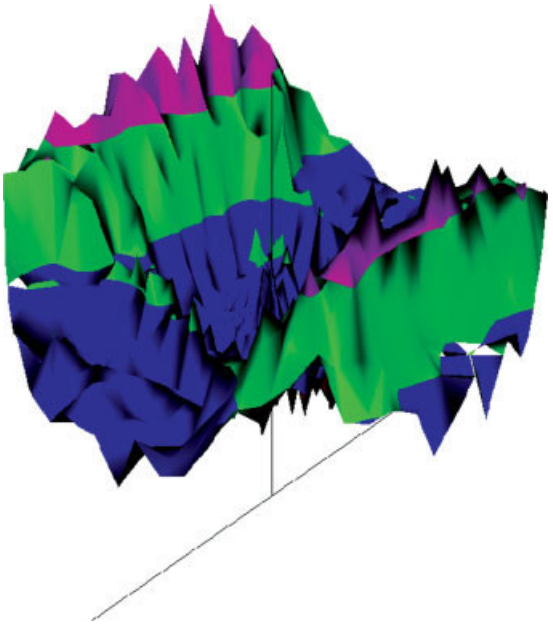

Figure 7 Three dimensional representation corresponding to Figure 6(c). [Color figure can be viewed in the online issue, which is available at www.interscience.wiley.com.]

ures maxima are observed in the SN direction and towards TD.

As indicated above, the angle between the (200) and (110) poles is 63°. The maxima in the (110) pole figure towards the TD are about 60° from SN, so it would be consistent with the *a* axis distribution in the SN. The *a* axis distribution at 35° to SN should produce maxima 82° from the SN, which would not be detected in Figures 5(b) and 6(b). The maximum observed in the SN direction, is possibly due to overlap from the intense (200) pole figure. The (110) pole figure for the uniaxially drawn samples [Fig. 6(b)] indicates that maxima lie in the SN/TD plane, implying that the *b* axes for the crystallites with the (200) maxima in the SN lie in the TD, so that, not surprisingly, *c* axes lie in the stretch direction (MD), following the amorphous polymer chains. The second crystallite distribution is one in which both *a* and *b* axes of the unit cell lie in the TD/SN plane, between these two axes, with c remaining in the MD. In the (111) pole figure there is a broad maximum in the SN/MD plane, approximately equidistant from each direction, but spreading in the TD direction. This is seen more clearly in the corresponding 3D representation, Figure 7. As seen in Table I, (201) and (210) planes which contribute to this peak are at 46° and 44° to the (200) planes respectively, so the crystallites with (200) planes in the SN direction could account for this peak. As explained previously, these reflections from the second distribution of crystallites will not be detected, lying beyond a χ angle of 70°. Also, the (111) plane is at an angle of 71° to the (200) plane, so neither first nor second

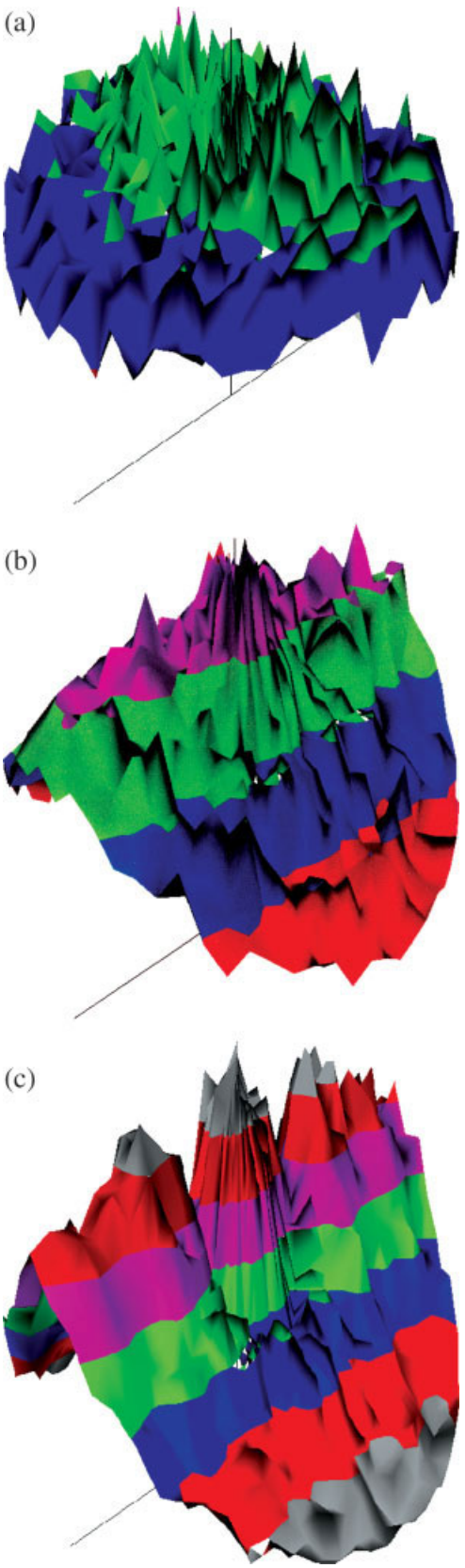

Figure 8 Three dimensional representation for 200 planes in (a) undrawn sample; (b) uniaxial DR = 2.0; (c) uniaxial DR = 3.0. [Color figure can be viewed in the online issue, which is available at www.interscience.wiley.com.]

distributions of crystallites will produce a detectable peak for these planes. In Table I the angles between (111), (210), (201), and (001) planes are listed. Although the (001) planes do not result in a diffraction peak, they do represent the *c* axis direction of the crystallites. Results for (111) and (201) planes are consistent with the *c* axis lying in the machine direction. For uniaxially drawn samples the original MD orientation has been removed during the drawing process.

The effect of draw ratio for uniaxial samples is illustrated in Figure 8. Clearly the two distributions of crystallite orientation both increase as draw ratio increases. The movement of (200) planes into the plane of the film also increases as biaxial draw ratio increases (Fig. 9). The increased orientation observed here correlates with improved mechanical properties.[10]

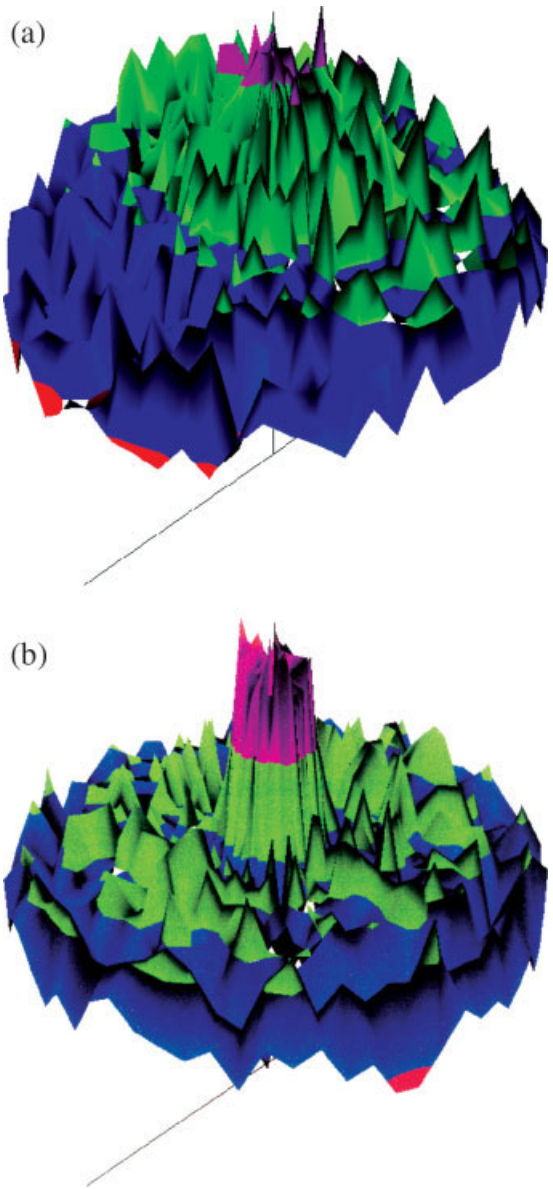

Figure 9 Three dimensional representation for 200 planes in (a) biaxial sample DR 1.5; (b) biaxial sample DR = 1.8. [Color figure can be viewed in the online issue, which is available at www.interscience.wiley.com.]

TABLE I
Interplanar Angles

Plane 1	Plane 2	Angle (°)
(200)	(110)	63
(200)	(111)	71
(200)	(210)	44
(200)	(201)	46
(001)	(111)	47
(001)	(210)	90
(001)	(201)	44

The 3D facility has enabled the second distribution to be investigated in more detail in uniaxially drawn films than previously,[11] and lead to a reinterpretation of this crystallite orientation. Guerrero[12] had also found that the second distribution of crystallites was present at a higher concentration in films drawn to a higher draw ratio, as is observed here. It is possible to provide a tentative explanation for this distribution by analogy with work previously reported for polyethylene.[15] Maddams and Preedy identified low and high stress crystallization orientation mechanisms. High stress crystallization produces a structure with the *c*-axis in the MD, and *a* and *b* axes randomly distributed as observed here. Possibly at higher DR *c* axis alignment is the driving force for crystallization, with little control over the orientation of *a* and *b* axes. Further work will be required to fully interpret these results.

CONCLUSIONS

Using modern XRD equipment incorporating a texture goniometer, the distribution of oriented crystallinity in a low crystallinity polymer such as PVC can be readily monitored, facilitating a better understanding of structural changes which occur. Results are consistent with those reported previously in that *a* axis orientation which can be obtained directly from the (200) pole figures is predominantly in the SN direction in biaxially oriented sheets, while two distributions of crystallite orientation are obtained for uniaxially drawn samples. However, substantially more information can be obtained than was possible previously, and uniaxially and biaxially oriented samples can be distinguished more easily. The evolution of orientation with increasing draw ratio has been observed.

References

1. Natta, G.; Corridini, P. J Polym Sci 1956, 20, 251.
2. Gray, A.; Gilbert, M. Polymer 1976, 17, 44.
3. Summers, J. W. J Vinyl Additive Technol 1981, 3, 107.

4. Mammi, M.; Nardi, V. Nature 1963, 199, 247.
5. Lebedev, V. P.; Okladov, N. A.; Minsker, K. S.; Shtarkman, B. P. Polym Sci (USSR) 1965, 7, 724.
6. Lebedev, V. P.; Okladov, N. A.; Shlykova, M. N. Polym Sci (USSR) 1967, 9, 553.
7. Gouinlock, E. V. J Polym Sci Polym Phys Ed 1975, 13, 961.
8. Gilbert, M. J Macromol Sci Polym Rev 1994, 34, 77.
9. Gilbert, M.; Hitt, D. J.; Harte, M. Plast Rubber Compos Process Appl 1994, 22, 177.
10. Gilbert, M.; Liu, Z.; Hitt, D. J Polym Eng Sci 1997, 37, 1858.
11. Gilbert, M.; Ross D. H.; Bowen, A. Polymer 1999, 40, 1233.
12. Guerrero, S. J. Polymer 1989, 38, 923.
13. Guerrero, S. J.; Meader, D.; Keller, A. J. Macromol Sci Phys 1981, 20, 185.
14. Cullity, B. D. Elements of X-ray Diffraction; Addison-Wesley Publishing: Reading, MA, 1967.
15. Maddams, W. F.; Preedy, J. E. J Appl Polym Sci 1978, 22, 2739.